JOURNAL OF OPTOELECTRONICS AND ADVANCED MATERIALS Vol. 9, No. 8, August 2007, p. 2376 - 2379

# Improving the detection accuracy in fiber Bragg grating sensors by using a wavelet filter

C. C. CHAN, N. NI*, J. SUN
*Blk. N1.3, Division of Bioengineering, School of Chemical and Biomedical Engineering, Nanyang Technological University, 70 Nanyang Drive, Singapore 637457*

Wavelet digital filter is designed and demonstrated to reduce the Bragg wavelength detection error in a fiber Bragg grating (FBG) strain sensor. Simulation and experimental results show that the wavelet filtering technique is a promising approach to enhance the measurement accuracy of the FBG strain sensor.

(Received May 21, 2007; accepted June 27, 2007)

*Keywords*: Fiber Bragg grating, Wavelet filter, Detection accuracy

## 1. Introduction

Over the past decade, strain sensing systems have become increasingly important in wide applications including geography, aerospace, structural monitoring, chemical and biomedical sectors. Optical fiber strain sensors outperform mechanical and other sensing counterparts with their specific features depending on the fibers themselves such as high sensitivity, low cost, light weight as well as immunity to electromagnetic interference [1]. Fiber Bragg gratings (FBGs), which are formed by coupling of light to the reverse-propagating guided mode, are proposed as simple yet versatile fiber strain sensors.

However, in order to measure strain variation with high accuracy, detection of the small shift in Bragg wavelength is essential. Several schemes have been reported for detecting the Bragg wavelength shift in FBG sensors [2, 3]. Among all the wavelength detection techniques, the most popular method is the peak detection technique, which uses a tunable laser source to scan through the spectrum of light reflected from the FBG and measure the wavelength corresponding to the maximum of intensity of the reflected light [4]. The peak detection technique can be applied to interrogate a number of FBG sensors based on wavelength division multiplexing (WDM) principle. However, the wavelength detection accuracy of the conventional peak detection technique is limited especially when the signal level of the reflected signal is low. Several signal processing methods, e.g., centroid detection algorithm coupled with curve fitting [5], spectrum correlation technique [6] and digital matched filter [7], have been proposed to improve the detection accuracy in this case.

In this paper, the use of digital wavelet algorithm to enhance the FBG strain measurement capability is reported. The principle and simulation are described in Section 2, followed by the experimental results which are given in Section 3. Finally, a conclusion is presented in the Section 4.

## 2. Principle and simulation

Computer simulation is carried out to demonstrate the effectiveness of digital filtering techniques for noise reduction in a FBG sensor system. The schematic diagram used in our simulation and experiment is shown in Fig.1. A narrow band tunable laser source (TLS) and optical spectrum analyzer (OSA) is used in the FBG sensing system. The laser light from the TLS is delivered, through a variable optical attenuator (VOA) and a 3dB directional coupler to the FBG, and the light reflected from the FBG is coupled back to the OSA through the same directional coupler. The FBG is held by a fixed stage (FS) and a translation stage (TS). Strain can be applied on the FBG by manually tuning the TS.

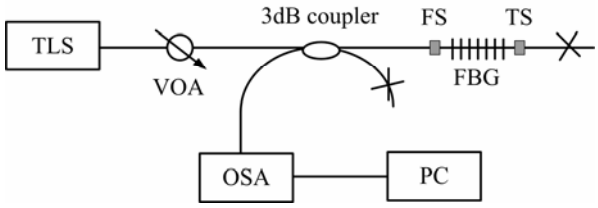


*Fig. 1. Schematic diagram of simulation and experimental setup. TLS: tunable laser source; VOA: variable optical attenuator; OSA: optical spectrum analyzer; FS: fixed stage; TS: translation stage; PC: personal computer; FBG: fiber Bragg grating.*

In the simulation, the reflection spectrum $R(\lambda)$ of a FBG with a Bragg wavelength $\lambda_B$ and a spectral full width at half-maximum (FWHM) symbolize as $\Delta\lambda_B$ is modeled as a Gaussian distribution [8] of

$$R(\lambda) = R_o \exp\left[-4\ln 2\left(\frac{\lambda-\lambda_B}{\Delta\lambda_B}\right)^2\right] \quad (1)$$

where $R_o$ is the maximum reflectivity that occurs at the Bragg wavelength. The spectrum of the reflected light at

the photodetector could be written as

$$I_s(\lambda)=\frac{I_o}{4}R(\lambda)=\frac{I_o}{4}R_o\exp\left[-4\ln 2\left(\frac{\lambda-\lambda_B}{\Delta\lambda_B}\right)^2\right] \quad (2)$$

where $I_o$ is the initial intensity of the light source, and the factor 1/4 is due to the 3-dB directional coupler.

When there is white Gaussian noise in the system, e.g. from the noise of the light source and/or environmental noise, the light intensity at the photodetector will, in addition to the ideal signal $I_s(\lambda)$, have a noise term $I_n(\lambda)$. Due to the existing of the noise, the combined signal will become

$$x(\lambda)=I_s(\lambda)+I_n(\lambda) \quad (3)$$

This will introduce the error for Bragg wavelength detection and reduce the measurement accuracy of the FBG sensor.

Wavelet transforms are found increasingly in speech and image processing applications. Their popularity lies in their non-block-based signal decomposition and multi-resolution processing properties which can be tailored for any application. The wavelet transform breaks a signal into shifts and translates of a basis function called a 'mother wavelet' which is a small wave of finite length. The time and scale shifts can be discretised to obtain what is known as the discrete wavelet transform (DWT), mathematically defined as follows [9]

$$\mathbf{\Psi}_{\tau,s}=\sum_{\tau,s}x(\lambda)\psi^*_{\tau,s}(\lambda) \quad (4)$$

where $x(\lambda)$ is the signal, $\psi(\lambda)$ is the mother wavelet. $\tau$ and $s$ are the shift and scale coefficients, respectively, and "*" represents complex conjugate.

The wavelet transformation could be functioned as a "filter" or known as wavelet denoising [10]. The method replies on the fact that noise commonly manifests itself as fine-gained structure in the signal, and the wavelet transform provides a scale-based N-level decomposition as illustrated as Fig. 2. The wavelet transforms are implemented in the form of filter banks. Each filter bank comprises a low-pass and a high-pass filter succeeded by a down-sampling by two. A number of filter banks are cascaded to produce a multi-resolution wavelet analysis.

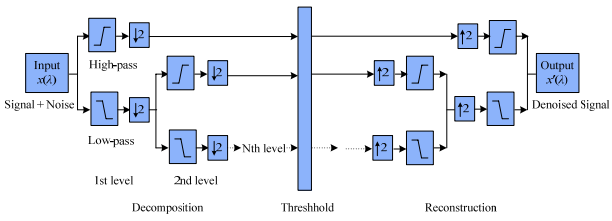


*Fig. 2. Block diagram for the DWT-based denoising scheme.*

After the decomposition, a threshold operation is applied. If the wavelet coefficients resulting from DWT are below the threshold, those components will be recognized as noises and be removed, then the reconstruction is performed by an inverse discrete wavelet transform (IDWT), so the denoised process is fulfilled.

Compared with the commonly used Fourier transform (FT), in which signals are represented as a sum of sinusoids, the highlights of the wavelets are: they could be localized in both time and frequency whereas the FT is only localized in frequency. Moreover, based on multi-resolution analysis, the wavelet processing provides better frequency and time resolution as signals are processed and analyzed at various scale [11].

A key question in the implementation of wavelet transforms is the choice of 'mother wavelet' function and the number of signal decomposition levels. Biorthogonal wavelet is selected to be used in this paper. Biorthogonal wavelet filters evolve from the idea of having an exact reconstruction scheme in which the synthesis filters are different from the analysis filters. Hence the 'orthonomality' condition is relaxed to 'biorthogonality' and implementation advantages in terms of linear phase filters and integer coefficients are possible [12].

Consider an ideal Gaussian reflection spectrum of an FBG sensor which is corrupted by additional of white noise. The FBG has a Bragg wavelength $\lambda_B$ of 1550nm, and a FWHM $\Delta\lambda_B$ of 0.2nm. The FBG spectrum with noise is sampled from 1549.5nm to 1550.5nm with a resolution of 1pm. The initial intensity of the laser source $I_o$ is 4pW and the maximum reflectivity that occurs at the Bragg wavelength is equal to 1. The contaminated signal, with a signal to noise ratio (SNR) of 3dB is realized by using a computer program.

The biorthogonal wavelet bior6.8 (6 and 8 are the orders of the decomposition or called analysis and reconstruction or called synthesis filters respectively) with a level of 5 is applied because it has short support and its symmetric filter coefficients have dyadic rational values enabling the simple arithmetic computation of inner products [13]. The ideal, contaminated and the estimated spectra after filtering are shown in Fig. 3. From the graph, the SNR after filtering increases dramatically compare with that before filtering, this demonstrates the promising potential to apply this filter to the contaminated FBG spectrum.

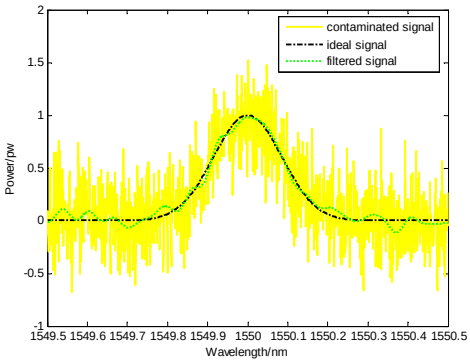


*Fig. 3. Ideal, contaminated and filtered reflection spectra.*

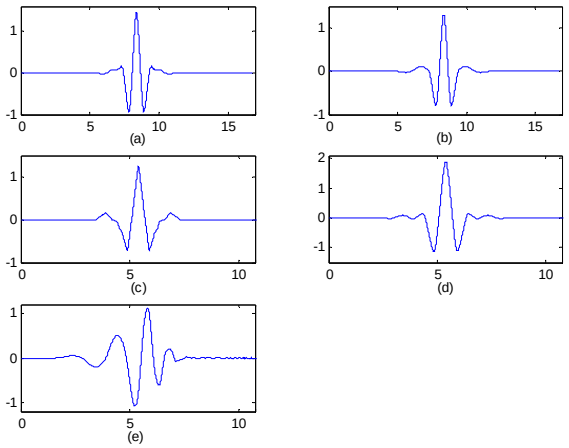


*Fig. 4. Wavelet functions: (a) decomposition wavelet of bior6.8, (b) reconstruction wavelet of bior6.8, (c) decomposition wavelet of bior 5.5, (d) reconstruction wavelet of bior5.5, (e) wavelet of db6.*

Because the noisy signal will be affected by the SNR and thus the performance of the filter at different SNR is investigated. Three types of wavelets bior 6.8, bior5.5 and Daubechies wavelet db6 with the same level are used, and their wavelet functions are as shown Fig. 4. The SNR of the white Gaussian noise is at the range of from 3dB to 30dB. After noise suppressing, the RMS error, which is defined by the RMS value of peak position difference between the filtered signal and the ideal signal, is computed to test the efficiency of the designed filter. The relationship of the error after filtering and the RMS of the noise are shown in Fig. 5(a). It can be seen that, with the increase of the SNR, the RMS error reduces gradually. From Fig. 5(a), the filtered errors of the bior5.5 and db6 wavelet filter both are larger than that of bior6.8, which shows the bior6.8 is a good choice in the FBG problem with the Gaussian noise.

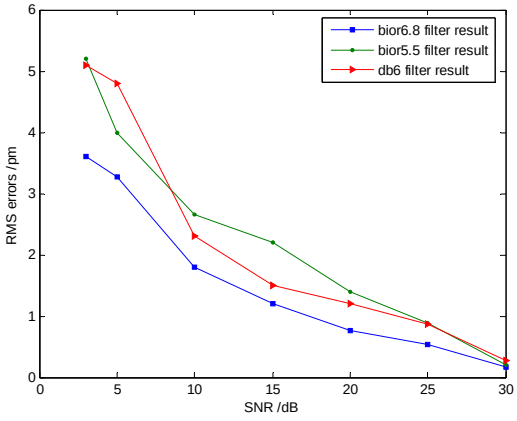


*Fig. 5(a). Relationship of the RMS error and SNR after filtering.*

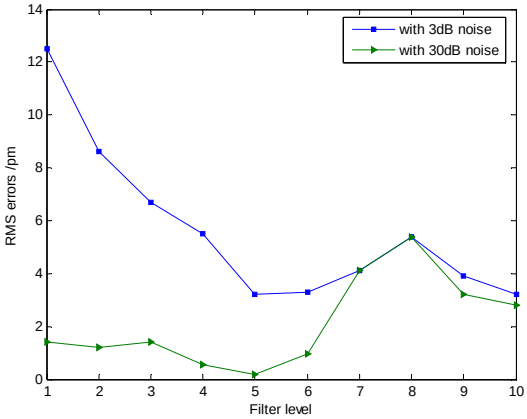


*Fig. 5(b). Relationship of the filter level and the RMS error after filtering.*

The relationship of the level of the bior6.8 filter and the RMS error after the filter is also investigated as shown in Fig. 5(b). It is shown that at level 5, minimum RMS error after the filtering is obtained at both the contaminated signal with high SNR of 30dB and low SNR of 3dB. The filter level is considered as the optimum level of the bior 6.8 filter, so the bior 6.8 filter with a filter level of 5 is selected to be applied on experimental results in the following part of the paper.

## 3. Experimental results

Experiments are conducted using the setup shown in Fig. 1. Light from the LED with the power about 30μW passed through a variable optical attenuator (VOA) and a 50/50 coupler and then was fed into a FBG. The reflected light from the FBG was guided back through the same coupler to an optical spectrum analyzer (OSA) that analyzed the reflected signal. The wavelength range of the OSA was set from 1549.5 to 1550.5 nm and sampled by 1000 points, corresponding to a step size of 1pm. The FBG was held by a fixed stage (FS) and a translation stage (FS). Strain could be applied on the FBG by manually tuning the TS. The 'ideal' reflection spectrum was measured by setting the VOA to 0 dB, which correspond to the large SNR. The noisy reflection spectrum was measured by setting the VOA to 20 dB, which effectively reduced the SNR value and thus gave rise to a noisy spectrum. The measurement was repeated for 10 times with 3minutes. Within this time period, the Bragg wavelength of the FBG could be regarded to be constant. The Bragg wavelength was only measured once for each strain step and the strain step used was 25 με. The reflection spectrum was changed to arbitrary unit for the convenience of analysis.

The errors varying with independent times and steps are investigated as in Fig. 6(a). The minimum error is achieved when the step is 10 at 6$^{th}$ measurement time, equal to 1pm. The corresponding original, contaminated and filtered spectra are shown in Fig. 6(b). It is clearly shown that the curve shape of the filtered signal is much closer to the original signal than the contaminated signal,

which proves the efficiency of the designed filter. The maximum error is 0.026nm when both of the step and the times are equal to 5. The corresponding filtered spectrum shown in Fig. 6(c) also demonstrates a more similar curve-shape to the original than the contaminated signal. But the wavelength has a relatively large error compared with the case in Fig. 6(b). This undesired error is due to the extremely high contamination of the noise to the spectral peak area. At this condition, the peak area of the signal is severely contaminated and thus the filter could not recognize the peak position correctly from the contaminated signal.

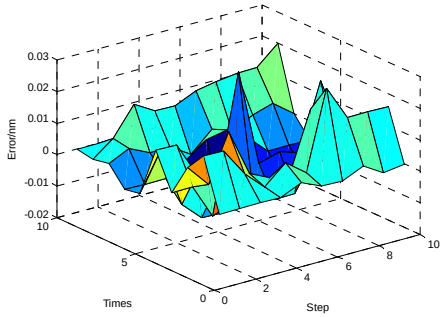


*Fig. 6(a). Relationship of measurement errors, measurement times and step of the applied strain.*

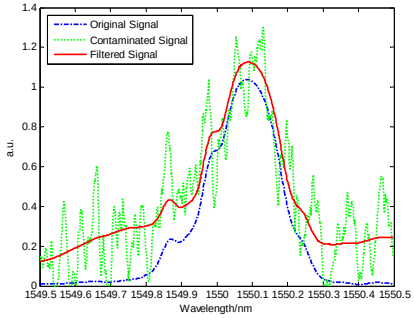


*Fig. 6(b). The ideal, contaminated and filtered spectra of the minimum Bragg wavelength detection error.*

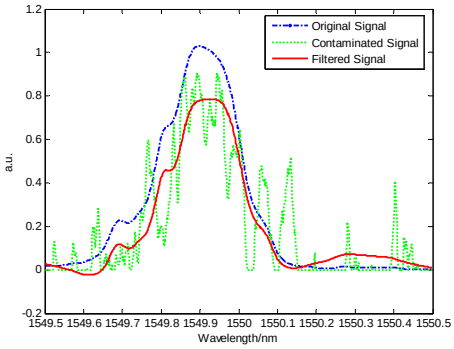


*Fig. 6(c). The ideal, contaminated and filtered spectra of the maximum Bragg wavelength detection error.*

## 4. Conclusion

A wavelet filter is applied to improve the measurement accuracy of a FBG sensing network. Simulation and experimental results show that, with proper wavelet function and filter level, the noise of the highly contaminated spectral signal could be successfully suppressed and a minimum Bragg wavelength detection error of 1pm is achieved after the filtering. However, the limitation of the wavelet filter should also be noticed. Normally, the higher level the filter is, the smoother the curve-shape of filtered signal will be. But with inappropriate large filter level, the signal will experience an over-filtering process and some information of the original signal will also be filtered. Furthermore, the retrieval of the signal is also limited by the SNR of the contaminated signal. A low SNR will make the wavelet filter fail to recognize the ideal signal from the noise, and the shape of the spectra and the corresponding central Bragg wavelength will be obtained incorrectly.

## References

[1] C. Wang, S. T. Scherrer, Optics Letters **29**(4), 352 (2004).
[2] A. Othonos, K. Kalli, Fiber Bragg gratings: fundamentals and applications in telecommunications and sensing, Artech House, Norwood, 1999.
[3] K. B. Rochford, S. D. Dyer, "Demultiplexing of interferometrically interrogated fiber Bragggrating sensors using Hilbert transform processing", IEEE/OSA Journal of Lightwave Technology **17**, 831 (1999).
[4] M. G. Xu, H. Geiger, J. P. Dakin, IEEE/OSA Journal of Lightwave Technology **14**, 391 (1996).
[5] A. Ezbiri, A. Munoz, S. E. Kanellopoulos, V. A. Handerek, IEE Colloq. Proceedings of IEE Colloquium on Optical Techniques for SMART Structures and Structural Monitoring (OTSMARTSSM'97) **33**, 5/1-5/6, (1997).
[6] J. M. Gong, C. C. Chan, W. Jin, J. M. K. MacAlpine, M. Zhang, Y. B. Liao, Optical Fiber Sensors Conference Technical Digest **1**, 155 (2002).
[7] C. C. Chan, J. M. Gong, C. Z. Shi, W. Jin, M. Zhang, L. M. Zhou, M. S. Demokan, Sensors and Actuators A, **104**, 19 (2003).
[8] C. C. Chan, W. Jin, M. S. Demokan, Optics &Laser Technology **31**, 299 (1999).
[9] Raghuveer M. Rao, Ajit S. Bogardikar, Wavelet transforms: introduction to theory and applications, Addison-Wesley Longman, Inc, 1998.
[10] Mark P. Wachowiak, Gregory S. Rash, Peter M. Quesada, Ahmed H. Desoky, IEEE Transaction on biomedical engineering **47**(3), 360(2000).
[11] G. Strang, T. Nguyen, Wavelets and filter banks, Wellesley-Cambridge Press, 1997.
[12] J. E. Odegard, C. S. Burrus, IEEE Digital Signal Processing Workshop Proceeding, pp. 73-76, (1996).
[13] S. Masud, J. V. McCanny, IEE Proceeding-Circuits, Devices and Systems, vol. **147**(5), 293 (2000).

*Corresponding author: nina@pmail.ntu.edu.sg